Amy Hall
NENG 612
8/29/2018

NENG 612 Foil Activation Project

Introduction

The original purpose of this project was to measure the neutron energy spectrum for the plutonium-beryllium (PuBe) source in the Air Force Institute of Technology (AFIT) graphite pile at the stinger two position. This was to be accomplished using foil activation analysis. In the post-irradiation processing, the foil activation data would have then been used to unfold the incident neutron spectra of the PuBe source within the AFIT pile. In order to accomplish the unfolding, the program STASYL, provided by Pacific Northwest National Laboratory (PNNL), could be utilized [3].

The initial project goals were updated after equipment failures prevented the irradiated foils from being measured using a High Purity Germanium (HPGe) Detector. The experimental data could not be obtained to complete the post-processing, which was one of the key objectives of the project. In place of the absent experimental data, supplementary foil data was provided which allowed for post-processing to calculate the activity immediately following irradiation. Additionally, data was provided to perform the energy and efficiency calibrations for the HPGe detector that was used to measure the activated foils.

The energy and efficiency calibration data that was provided was from ^{241}Am, ^{133}Ba, ^{60}Co, ^{151}Eu and ^{137}Cs sources. The foil activation data provided was from Al, Ni, In and Au foils. In order to perform the energy calibration, the program Peak Easy was used [4]. One consideration for the calibration data was that the sources were measured 18 cm from the detector whereas the foils were measured only 1 cm from the detector due to their low activity. This required correction factors to be used for each of the activated foils in order to correct for the variation in distance between the calibration data and the foil data. These correction factors were also provided.

The primary objective for this project after the difficulties that arose was to use provided data from a foil activation experiment to perform post-processing work. The initial foil

activation experiment efforts will be discussed without results. Next, the provided calibration and foil data will be introduced. Methodology and results will be provided for the foil activation data to include the energy and efficiency calibrations, geometric efficiency and solid angle considerations, and a final determination of the time-zero activity of the activated foils.

Description of Work

The foils were stacked on top of each other in the configuration shown in figure 1. The foils were all roughly the same diameter between with the exception of the Al foils which was larger. The thicknesses of the foils were all between 0.002in and 0.077in.

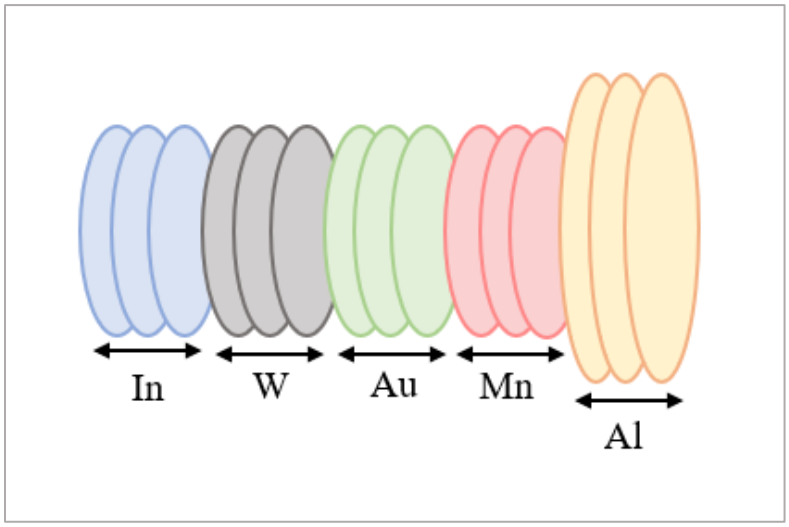

Figure 1: Diagram of stacked activation foils showing the order they were placed in the graphite Pile. The indium foils were placed closest to the source.

The foil stack was placed in stringer 2 of the AFIT Building 470 graphite pile and the PuBe source was placed above it as shown in figure 2. The foil activation was originally scheduled for 7 days but was increased to 10 days to fit into scheduling constraints unrelated to the project. The foil activation process was not inhibited by the additional irradiation time.

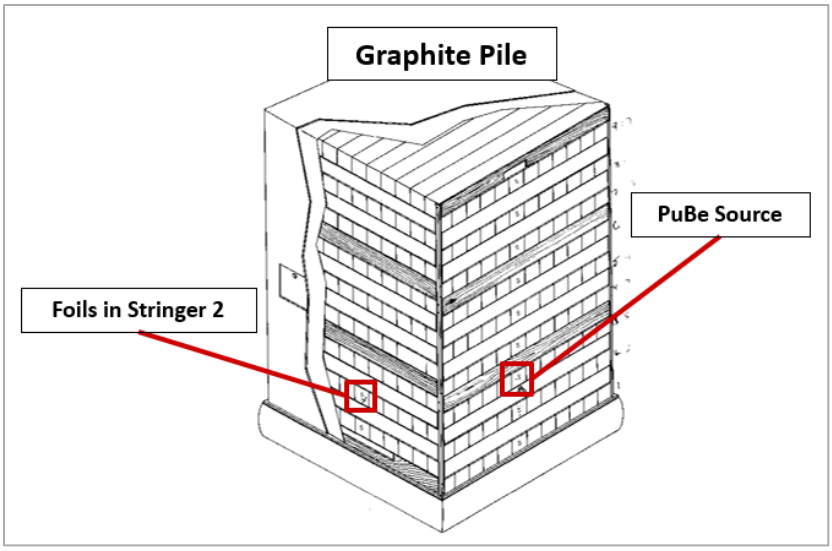

Figure 2: Graphite pile diagram with foil and PuBe source locations marked.

During the foil irradiation, an HPGe detector was calibrated using a known-multi-nuclide source at 4 and 2 cm from the detector face. In the middle of the calibration process, the detector and computer system shutdown and remained inoperable through several rounds of troubleshooting. ~~All of t~~The other AFIT Building 470 HPGe detectors were unable to be used~~also inoperable~~. Two portable HPGe detectors were available; however, one was non-operational, and they did not have sufficient storage, efficiency and operating time capabilities to measure the activated foils. Therefore, the experiment transitioned to a data post-processing analysis with the provided data rather than the data from the foils that were irradiated.

For the calibrations, the pulse height spectrum data was provided from ^{241}Am, ^{133}Ba, ^{60}Co, ^{151}Eu, and ^{137}Cs. To perform the calibration, each of the decay lines shown in Table 1 were fitted using Peak Easy to determine the total counts in the gamma ray peak. The standard Gaussian fits with a linear background were edited manually to provide the best fit based on estimating the background and minimizing the reduced chi-squared value that Peak Easy provides. Once a good fit is determined, Peak Easy provides the peak centroid channel required for the energy calibration and the net peak area and peak area uncertainty required for the efficiency calibration. In some cases, the peak curves are best described by more than one Gaussian. In order to propagate the uncertainty for the energy spectra calibrations when dealing with multiple Gaussian curves, equation 1 must be used.

$$\delta R = \sqrt{\delta X^2 + \delta Y^2 + \delta Z^2} \qquad (1)$$

This equation is applicable when adding quantities together that each have uncertainties.

The known energies of the gammas can be fit to the reported peak centroid channel numbers using a first-order least-squares fit of the data. This can be used to determine the energies of the resultant gammas emitted from the activated foils to precisely identify gammas associated with different activation products.

Efficiency calibrations are used to compare detectors. When the efficiency of a detector is known, it can be used to estimate the absolute efficiency of the source. The efficiency of the detector is calculated by considering the initial source activity and accounting for how much of the activity decayed away based on the age of the source and the source decay constant. Once the updated activity is known, the geometric efficiency of the detector must be considered which is based on the solid angle between the source and the detector. Next, the source branching ratios are considered to determine the likelihood of the source decaying by given processes. This information can be combined to provide the number of expected counts for each gamma ray peak. The measured number of counts is divided by this number to provide the efficiency at a given energy. Equation 2 provides a general equation for efficiency in terms of energy that can be used as a basis for efficiency calibration.

$$\ln(\epsilon) = \sum_{i=1}^{N} a_i \left(\ln\left(\frac{E}{E_0}\right)\right)^{i-1} \qquad (2)$$

where ϵ is the efficiency, E is the gamma-ray energy, and a_i and E_0 are fitted parameters. Python was used in this experiment to perform a curve-fit in order to produce the calibration equation based on energy and efficiency calibrations. This equation was then used in the time-zero calculation for the activated foils.

Ideally sources measured with an HPGe will be taken from far enough away to be considered a point source. However, that is not always possible and, in those situations, the solid angle of the source with respect to the detector must be considered. In the case of this experiment a solid angle calculation was made to determine whether the calibration sources, which were measured 18 cm from the detector face, can be considered to be point sources. Equation 3 calculates the emission rate for a point source.

$$S = N\frac{4\pi}{\epsilon_{dip}\Omega} \qquad (3)$$

Equation 4 shows how the solid angle can be calculated for sources that can be considered point sources. This equation is an approximation that can be made as long as d (the distance from the detector) is larger than a (the detector radius) which is true in the case of this experiment.

$$\Omega \cong N\frac{\pi a^2}{d^2} \qquad (4)$$

For sources that cannot be approximated as a point source, equation 5 must be used.

$$\Omega \cong 2\pi\left[1 - \frac{1}{(1+\beta)^{\frac{1}{2}}} - \frac{3}{8}\frac{\alpha\beta}{(1+\beta)^{\frac{5}{2}}} + \alpha^2[F1] - \alpha^3[F2]\right]$$

$$F1 = \frac{5}{16}\frac{\beta}{(1+\beta)^{7/2}} - \frac{35}{16}\frac{\beta^2}{(1+\beta)^{9/2}}$$

$$F2 = \frac{35}{128}\frac{\beta}{(1+\beta)^{9/2}} - \frac{315}{256}\frac{\beta^2}{(1+\beta)^{11/2}} + \frac{1155}{1024}\frac{\beta^2}{(1+\beta)^{13/2}}$$

$$\alpha \equiv \left(\frac{a}{d}\right)^2 \qquad \beta \equiv \left(\frac{s}{d}\right)^2 \qquad (5)$$

where a is the radius of the detector, s is the source radius and d is the distance between the source and the detector. Equation 4 and 5 will be used in this experiment to determine whether the calibration sources can be considered point sources (at 18cm from the detector) or if the approximation is not appropriate in this case. Correction factors were provided for this experiment to account for this. However, the calculation will still be made as an example of the applicable methodology.

The pulse height spectrum data was provided for activated In, Ni, Au, and Al foils. The reactions of interest that were used for these foils were: $^{27}\mathrm{Al}(n,p)^{27}\mathrm{Mg}$, $^{27}\mathrm{Al}(n,\alpha)^{24}\mathrm{Na}$, $^{58}\mathrm{Ni}(n,2n)^{57}\mathrm{Ni}$, $^{115}\mathrm{In}(n,n')^{115\mathrm{M}}\mathrm{In}$, $^{115}\mathrm{In}(n,\gamma)^{116}\mathrm{In}$, $^{197}\mathrm{Au}(n,2n)^{196}\mathrm{Au}$ and $^{197}\mathrm{Au}(n,\gamma)^{196}\mathrm{Au}$. In order to calculate the initial time-zero activity for the activated foils, equation 6 was utilized. This equation must be adjusted for the decay between irradiation and measurement.

$$A_0 = \frac{C\lambda e^{\lambda\Delta t_j}}{(1-e^{-\lambda\Delta t_C})\epsilon(E_\gamma)f_l I_\gamma} \qquad (6)$$

A_0 is the initial activity of the measured radiation source at creation, C is the number of counts measured using the detector, λ is the decay constant associated with the gamma ray, Δt_j is the

time between the end of irradiation and the beginning of counting, Δt_c is the total count time, $\epsilon(E_\gamma)$ is the detector efficiency for a given decay line, f_l is the detector live-time fraction, and I_γ is the gamma intensity [2]. The efficiency for given decay lines is found using the efficiency calibration equation developed previously. Additionally, this calculation required the use of the provided correction factors in the numerator to account for different measurement distances between the calibration and activated foil measurement.

Results

The calibration data was fit using Peak Easy as described in the Methodology section. An example fit for the 661.657 keV gamma ray peak of ^{137}Cs is provided below in figure 3. In this example, the best fit was made using a quadratic function with two Gaussian curves.

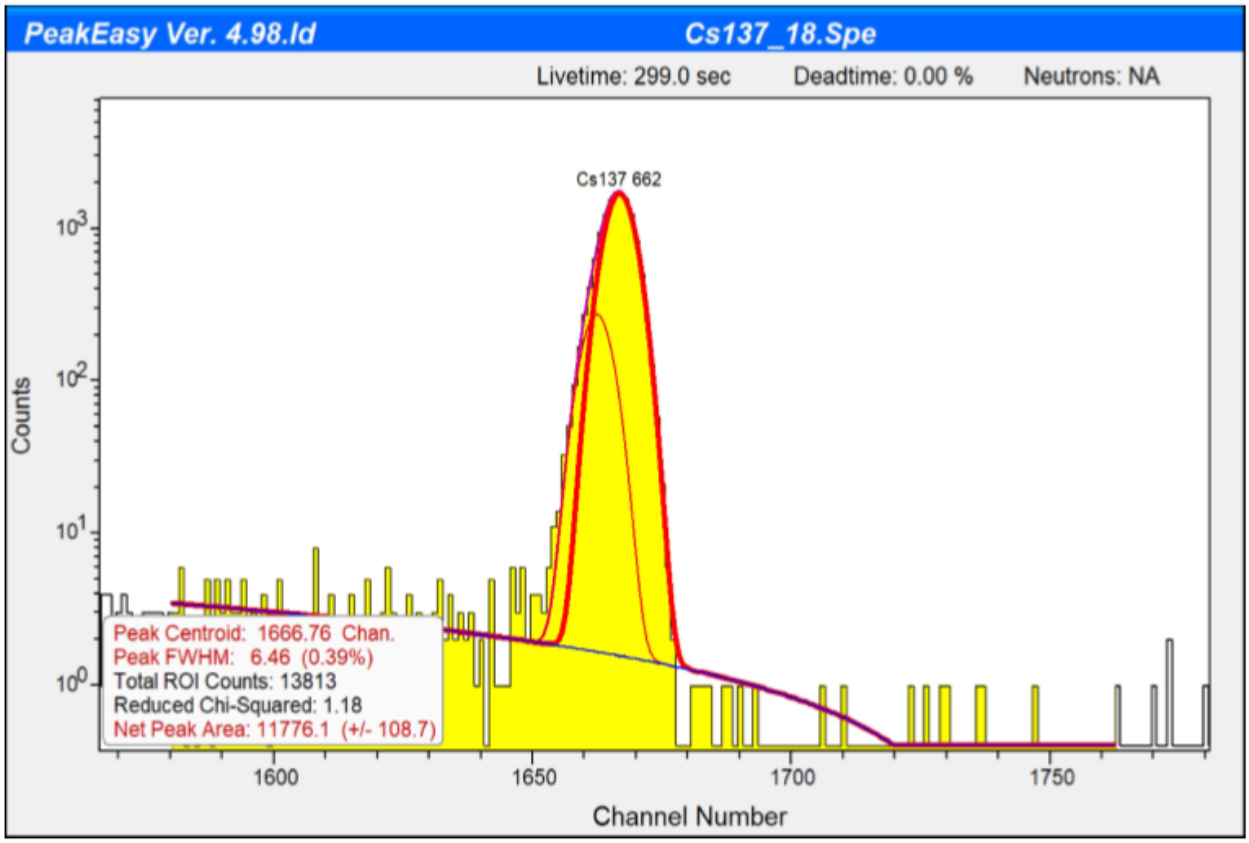

Figure 3: Cs-137 661.7 keV gamma ray peak analysis in Peak Easy

Table 1 shows the peak counts and chi-squared (χ^2) values for each of the calibration peaks used.

Isotope	Energy [keV]	Peak Area [counts]	Reduced χ^2
^{241}Am	59.5409	45745.9	9.5
^{152}Eu	121.7	85082.7	2.76
^{152}Eu	244.7	15624.2	1.50
^{133}Ba	302.85	24189.1	2.10
^{152}Eu	344.38	40954.9	2.29
^{133}Ba	356.01	72242.7	4.96
^{137}Cs	661.657	13667.5	1.18
^{152}Eu	778.9	1006.2	1.53
^{152}Eu	964.06	9624.2	1.25
^{152}Eu	1085.837	7212.3	1.29
^{152}Eu	1112.08	8021.1	1.38
^{60}Co	1173.23	11231.5	1.98
^{60}Co	1332.49	11231.5	1.97
^{152}Eu	1408.01	10610.4	1.74

Table 1: Energy, peak area and χ^2 values for the calibration peaks.

The χ^2 value were able to be kept low with the exception of the ^{241}Am peak and the ^{133}Ba 356.01 keV energy peak. For the ^{241}Am peak in particular, the higher than desired χ^2 value was less concerning because it was on the lower end of the energy range which did not need to have as good of a fit since the provided foil activation data was above this energy range.

The detector efficiency calibration was performed using Python as discussed in the Methodology section. Figure 4 displays a plot of the calibration curve which was fitted using a curve fit tool on Python. The experimental data used for the calibration is also displayed.

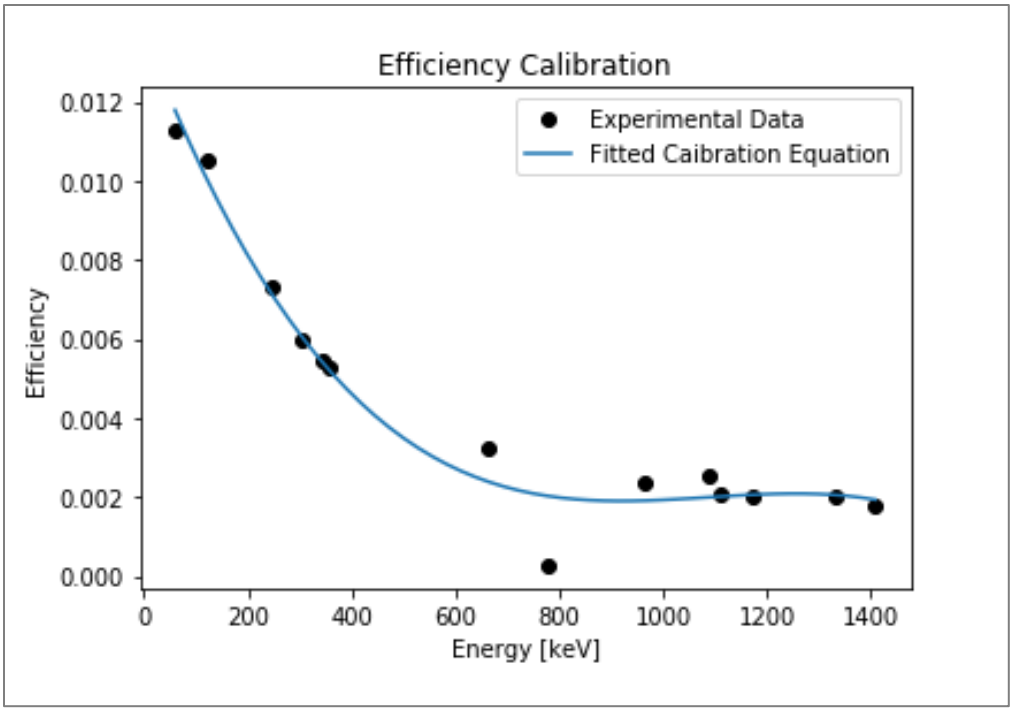

Figure 4: Detector efficiency versus energy plot with original experimental data and fitted calibration curve.

Equation 7 is the calibration equation that was produced from the experimental data. The graph of this equation is plotted in figure 4 along with the experimental data.

$$\epsilon = 9.833 \times 10^{-12}(E) + 3.205 \times 10^{-8}(E) + 3.398 \times 10^{-5}(E) + 0.0137 \qquad (7)$$

This calibration equation was used in the calculation of the time-zero calculations for the foils as described in the Methodology section.

The solid angle for the 18 cm energy calibration sources were found using the point source estimation equation as well as the equation for sources which cannot be considered point sources. This process was discussed in the Methodology section. The solid angle calculated from the point source estimation (equation 4) was 0.0582 radians (fractional angle percent 0.0046) and the solid angle calculated with equation 5 was 0.0566 radians (fractional angle percent 0.0045). The solid angles calculated in these two methods are very similar which means that it was appropriate to estimate the calibration sources as point sources when they are 18cm from the detector.

The time-zero activity was calculated for each of the activated foils based on designated decay lines as described in the Methodology section. The results of these calculations are shown in table 2.

Reaction	Decay Line Energy (keV)	Time-Zero Activity (A_0) [μCi]
$^{115}\mathrm{In}(n,n')^{115\mathrm{M}}\mathrm{In}$	336.241	0.051580904
$^{115}\mathrm{In}(n,\gamma)^{116}\mathrm{In}$	1293.4	0.244372386
$^{58}\mathrm{Ni}(n,2n)^{57}\mathrm{Ni}$	1377.63	0.000751185
$^{197}\mathrm{Au}(n,\gamma)^{196}\mathrm{Au}$	355.7	0.001543732
$^{197}\mathrm{Au}(n,2n)^{196}\mathrm{Au}$	411.8	0.001093973
$^{27}\mathrm{Al}(n,p)^{27}\mathrm{Mg}$	843.76	0.106712737
$^{27}\mathrm{Al}(n,\alpha)^{24}\mathrm{Na}$	1368.63	0.011865505

Table 2: Time-zero activity calculations for given decay lines for the activated foils.

The time-zero activity calculations were done using equation 6. The given decay lines were chosen based upon the correction factors that were provided.

Conclusion

The original goals for this project were to perform a foil activation experiment in order to characterize the AFIT building 470 graphite pile and PuBe neutron source. A secondary goal was to perform the necessary post processing work associated with this process in order to gain familiarization with the methodology. Due to issues that arose with the available equipment required for the experiment, the goals had to be adjusted and the original goal of measuring the graphite pile PuBe source was unable to be completed. The foil activation experiment was performed up through the post-processing work. Data was then provided which allowed for post-processing to still be completed to achieve the secondary goal associated with this project. Using the data that was provided, energy and efficiency calibrations were completed for the detector used to produce the data. Foil activation data was also provided which was used to characterize the activated foils in order to determine the zero-time activity of the foils.

REFERENCES

[1] G. F. Knoll Radiation Detection and Measurement Hoboken, NJ: John Wiley and Sons, Inc., 2010.

[2] N. Munshi and Z. Sweger, “33MeV and ETA Activation Analysis,” 2017.

[3] Pacific Northwest National Laboratory. “More Information About the STAYSL PNNL Suite.” *In Situ Bioremediation*, bioprocess.pnnl.gov/STAYSL_PNNL_Request.htm.

[4] Los Alamos National Laboratory. “Welcome to PeakEasy Home Page.” *Peakeasy.lanl.gov*, peakeasy.lanl.gov/.